THE JOURNAL OF BIOLOGICAL CHEMISTRY VOL. 288, NO. 24, pp. 17769–17781, June 14, 2013

Role of Central Metabolism in the Osmoadaptation of the Halophilic Bacterium *Chromohalobacter salexigens*[*] [S]

Received for publication, March 18, 2013, and in revised form, April 8, 2013 Published, JBC Papers in Press, April 24, 2013, DOI 10.1074/jbc.M113.470567

José M. Pastor[‡1,2], Vicente Bernal[‡1,3], Manuel Salvador[§2], Montserrat Argandoña[§4], Carmen Vargas[§], Laszlo Csonka[¶5], Ángel Sevilla[‡6], José L. Iborra[‡], Joaquín J. Nieto[§], and Manuel Cánovas[‡7]

From the [‡]Departamento de Bioquímica y Biología Molecular B e Inmunología. Facultad de Química, Campus Regional de Excelencia Internacional "Campus Mare Nostrum," Universidad de Murcia, 30100 Murcia, Spain, the [§]Departamento de Microbiología y Parasitología, Universidad de Sevilla, 41012 Seville, Spain, and the [¶]Department of Biological Sciences, Purdue University, West Lafayette, Indiana 47907-2064

Background: *Chromohalobacter salexigens* synthesizes and accumulates ectoines.
Results: High ratio of the anaplerotic and catabolic fluxes involved in ectoines synthesis supports high biosynthetic fluxes at high salinity and leads to metabolite overflow at low salinity.
Conclusion: Evolution optimized the metabolism of *C. salexigens* to support high production of ectoines.
Significance: Metabolic adaptations in a compatible solute-accumulating halophile are described for the first time.

Bacterial osmoadaptation involves the cytoplasmic accumulation of compatible solutes to counteract extracellular osmolarity. The halophilic and highly halotolerant bacterium *Chromohalobacter salexigens* is able to grow up to 3 M NaCl in a minimal medium due to the *de novo* synthesis of ectoines. This is an osmoregulated pathway that burdens central metabolic routes by quantitatively drawing off TCA cycle intermediaries. Consequently, metabolism in *C. salexigens* has adapted to support this biosynthetic route. Metabolism of *C. salexigens* is more efficient at high salinity than at low salinity, as reflected by lower glucose consumption, lower metabolite overflow, and higher biomass yield. At low salinity, by-products (mainly gluconate, pyruvate, and acetate) accumulate extracellularly. Using [1-^{13}C]-, [2-^{13}C]-, [6-^{13}C]-, and [U-$^{13}C_6$]glucose as carbon sources, we were able to determine the main central metabolic pathways involved in ectoines biosynthesis from glucose. *C. salexigens* uses the Entner-Doudoroff pathway rather than the standard glycolytic pathway for glucose catabolism, and anaplerotic activity is high to replenish the TCA cycle with the intermediaries withdrawn for ectoines biosynthesis. Metabolic flux ratios at low and high salinity were similar, revealing a certain metabolic rigidity, probably due to its specialization to support high biosynthetic fluxes and partially explaining why metabolic yields are so highly affected by salinity. This work represents an important contribution to the elucidation of specific metabolic adaptations in compatible solute-accumulating halophilic bacteria.

Halophilic microorganisms demand relatively high salt concentrations to grow. Because of the diversity of environments where they can thrive, their physiology is widely varied. The metabolic diversity of halophilic and halotolerant microorganisms is conditioned by the adaptation to specific environmental niches (especially evident in the case of alkalophilic, methanotrophic, or thermophilic halophilic bacteria) and also by osmoadaptation mechanisms that these microorganisms developed to cope with salinity (1–3). As a consequence, the preferred metabolic pathways used to assimilate carbon sources are also diverse.

Strategies of osmoadaptation can be roughly classified in two main types. The "salt-in" strategy, which consists of the accumulation of K^+ and Cl^- in the cytoplasm of the cells, is used by extremely halophilic aerobic archaea, halophilic fermentative bacteria, and the extremely halophilic bacterium *Salinibacter ruber* (4–6). The "organic solutes-in" strategy, which involves the accumulation of organic "compatible" solutes, is used by a larger variety of organisms, including all mesophilic bacteria, halophilic algae, halophilic methanogenic archaea, and halotolerant and halophilic aerobic bacteria (7). Among the halophilic eubacteria that use the organic solutes-in strategy, strict aerobiosis is more frequent because compatible solute synthesis is energetically and metabolically a very demanding process (4). Compatible solutes belong to a few chemical families: sugars (sucrose and trehalose), polyols (glycerol, glucosylglycerol, mannosylglycerol, and arabitol, among others), amino acids (glutamine and derivatives, proline, alanine), quaternary amines (betaines and choline), and ectoines (ectoine and β-hydroxyectoine). Ectoine is one of the most widely distributed

* This work was supported in part by Fondo Europeo de Desarrollo Regional funds, Ministerio de Ciencia e Innovación (Spain) Projects BIO2008-04502-01, BIO2011-29233-C02-01, and BIO2011-22833, Junta de Andalucía (Spain) Grant P08-CVI-03724, and Spanish National Network on Extremophilic Microorganisms Grant BIO2011-12879-E.
[S] This article contains supplemental Materials and Methods, Tables S1–S4, Figs. S1–S8, and additional references.
[1] Both authors contributed equally to this work.
[2] Recipient of Formación de Profesorado Universitario and Formación de Personal Investigador fellowships from MICINN (Spain).
[3] Recipient of a post-doctoral contract from Universidad de Murcia (Programa Propio). To whom correspondence may be addressed: Grupo de Bioenergía, Dirección de Tecnología, Centro de Tecnología de Repsol, Carretera A-5, Km 18, 28935 Móstoles-Madrid, Spain. Tel.: 34-868-887393; Fax: 34-868-884148; E-mail: vbernal@um.es.
[4] Recipient of a post-doctoral contract from Junta de Andalucía.
[5] Supported by National Science Foundation Award IOS-1054977.
[6] Recipient of a post-doctoral contract from the Programa Juan de la Cierva (Spain).
[7] To whom correspondence may be addressed. Tel.: 34-868-887393; Fax: 34-868-884148; E-mail: mcanovas@um.es.

compatible solutes. Hydroxyectoine is often synthesized at lower amounts together with ectoine by many ectoine-producing species (8). When present in the medium, either these compounds or their precursors can be taken up from the environment. When cells are growing in media lacking compatible solutes, these compounds can only be accumulated by *de novo* synthesis (9).

Chromohalobacter salexigens DSM 3043 (formerly *Halomonas elongata* DSM 3043) is a halophilic γ-proteobacterium of the family Halomonadaceae (10). It has one of the widest salinity ranges for growth found in nature (10, 11). In *C. salexigens*, osmoadaptation is mainly achieved by the accumulation of ectoine and hydroxyectoine (designated together as "ectoines") (9). The biosynthetic pathway for ectoines was established in *H. elongata* and *C. salexigens* (11–15).

The availability of the genomic sequence of *C. salexigens* (16) presents an opportunity for the understanding of the characteristic metabolic features of this halophile and their relevance for osmoadaptation. During active growth, metabolite fluxes are substantially directed toward biosynthetic pathways, draining intermediaries of central metabolism. Therefore, the perfect coupling and efficiency of the metabolic pathways linking carbon sources to the end products (in our case, compatible solutes) is crucial. There are two major pathways for the catabolism of sugars to pyruvate: glycolysis (Embden-Meyerhof pathway) (EM)[8] and the Entner-Doudoroff (ED) pathway (17). The physiological relevance of these pathways for the growth of *C. salexigens* is not known (16, 18, 19). The synthesis of ectoines consumes acetyl-CoA, which is produced by oxidative decarboxylation of pyruvate, and oxaloacetate (OAA), which is an intermediate in the TCA cycle and has to be replenished by anaplerotic pathways (16). The flux ratios between anaplerotic and catabolic pathways are highly relevant for metabolic adaptation.

Metabolic studies in halophilic and halotolerant bacteria are scarce, especially if a focus on the biosynthesis of compatible solutes is sought. In this work, we gained new insights into the role of central metabolism in the osmoadaptation of *C. salexigens*. Using isotope label tracing, we analyzed the pathways for glucose catabolism and how central metabolism copes with the high metabolic burden caused by ectoines biosynthesis. Our results show how the adaptations developed by this bacterium affect metabolic efficiency at different salinities and represent a step further in the understanding of the physiology of halophilic and halotolerant bacteria.

MATERIALS AND METHODS

Bacterial Strains and Cultures

C. salexigens CHR61, a rifampicin-resistant spontaneous mutant of *C. salexigens* DSM 3043^T, was used throughout this study. For ectoine production and for characterization of metabolic pathways, the strain was grown in minimal medium M63 (pH 7.2) containing 16.3 g/liter KH_2PO_4, 4.2 g/liter KOH, 2 g/liter $(NH_4)_2SO_4$, 39.5 mg/liter $MgSO_4{\cdot}7H_2O$, 0.5 mg/liter $FeSO_4{\cdot}7H_2O$. M63 was supplemented with 35.0, 43.8, 146.0, or 175.2 g/liter NaCl (corresponding to 0.6, 0.75, 2.5, or 3 M). As a carbon source, 20 mM glucose was used. Aerobic 100-ml batch cultures were grown in 0.5-liter flasks at 37 °C on a rotary shaker at 210 rpm.

Cultures were started from frozen 20% glycerol stocks. Precultures were grown in SW-2 medium (containing 2% (w/v), or 0.3 M, total salts) composed of 15.6 g/liter NaCl, 4.07 g/liter $MgSO_4{\cdot}7H_2O$, 2.6 g/liter $MgCl_2{\cdot}6H_2O$, 0.4 g/liter KCl, 67 mg/liter $CaCl_2{\cdot}2H_2O$, 47 mg/liter NaBr, and 13 mg/liter $NaHCO_3$ (20). M63 cultures were inoculated to an initial absorbance (A_{600}) of 0.025 with an exponential phase preculture grown overnight in SW-2 medium. Glycerol stocks, solid culture media, and precultures were supplemented with rifampicin to a final concentration of 25 μg/ml.

Analytical Procedures

Cell Growth—To measure cell concentration, cells were resuspended in a NaCl solution (0.6 to 3.0 M), and absorbance was measured at 600 nm (Novaspec Plus Visible Spectrophotometer, Amersham Biosciences). A_{600} and gram of dry cell weight (g_{DCW}) were correlated for the strain used, according to the following empirical equations: $g_{DCW}/liter = 0.597{\cdot}A_{600}$ (for 0.6 M grown cultures), $g_{DCW}/liter = 0.557{\cdot}A_{600}$ (for 0.75 M grown cultures), and $g_{DCW}/liter = 0.532{\cdot}A_{600}$ (for 2.5 and 3 M grown cultures).

Determination of Extracellular Organic Acids—Extracellular organic acids were determined by ion exchange chromatography. Acetate was analyzed in a Shimadzu LC-10 HPLC instrument (Shimadzu Scientific Instruments, Columbia, MD), equipped with differential refractive index and diode array (UV) detectors (Shimadzu Scientific Instruments, Columbia, MD). A cation exchange HPX-87H column (Bio-Rad) was used for the separation of organic acids. The mobile phase was 5 mM H_2SO_4 at a 0.5 ml·min^{-1} flow rate and 45 °C. Gluconate (*m*/*z* 195), pyruvate (*m*/*z* 87), lactate (*m*/*z* 89), and citrate (*m*/*z* 191) were measured using HPLC-MS. Analysis was performed with an Agilent 1200 series HPLC instrument (Agilent Technologies, Santa Clara, CA) coupled to an Agilent 6120 single quadrupole mass spectrometer with orthogonal electrospray ionization source. The mass spectrometer was operated in the negative electrospray ionization mode, using the SCAN mode at a range of *m*/*z* 50–300, whereas the selected ion monitoring mode was used for the *m*/*z* of each compound. The ion spray voltage was set at 3500 V. Nitrogen with a flux of 12 liters/min was used as the sheath gas (40 p.s.i.) and the auxiliary gas. The ion transfer capillary was heated to 350 °C. The fragmentation voltage was set at 70 V. Separation was carried out on an injection volume of 10 μl using the same column and conditions as the previous method, substituting 5 mM H_2SO_4 with 0.1% formic acid. Data were acquired by a PC using the Agilent Chemstation software.

Isotopic Labeling Studies and NMR Spectroscopy—For the labeling experiments, cells were grown in 100 ml of M63 medium in the presence of isotopically labeled glucose (Cortec-

[8] The abbreviations used are: EM, Embden-Meyerhof; ED, Entner-Doudoroff; OAA, oxaloacetate; Gdh, glutamate dehydrogenase; Pc, pyruvate carboxylase; Ppc, phosphoenolpyruvate carboxylase; Icdh, isocitrate dehydrogenase; Cs, citrate synthase; Pfk, 6-phosphofructokinase; Gdh, glutamate dehydrogenase; PEP, phosphoenolpyruvate; Pdh, pyruvate dehydrogenase.

TABLE 1

Growth and production of ectoines of *C. salexigens* at different NaCl concentrations

Cultures were grown at 37 °C in M63 minimal medium with 20 mM glucose and 30 mM ammonium as the sole carbon and nitrogen sources (see "Materials and Methods" for details).

NaCl concentration in medium	Maximum biomass	$Y_{Ect/X}$ [a]	Ectoines production rate	Hydroxyectoine/ectoine ratio
	$g_{DCW}{\cdot}liter^{-1}$	$mmol{\cdot}g_{DCW}{}^{-1}$	$mmol{\cdot}(g_{DCW}{\cdot}h)^{-1}$	
0.6 M	1.40 ± 0.07	0.18 ± 0.01	0.049 ± 0.003	0.048 ± 0.097
0.75 M	1.76 ± 0.03	0.45 ± 0.01	0.127 ± 0.004	0.106 ± 0.030
2.5 M	2.48 ± 0.02	1.10 ± 0.05	0.174 ± 0.008	0.507 ± 0.037
3 M	2.03 ± 0.26	1.68 ± 0.09	0.159 ± 0.009	0.423 ± 0.036

[a] Stoichiometric coefficient of ectoines production. $Y_{Ect/X}$ and ectoines production rates were determined in the exponential phase of cultures. Maximum biomass and hydroxyectoine to ectoine ratio were obtained in the early stationary phase.

Net, Voisins-Le Bretonneux, France). Isotopically labeled substrates used were 100% [1-^{13}C]-, [2-^{13}C]-, [6-^{13}C]glucose, or 20% [U-$^{13}C_6$]glucose. Cultures were harvested in the mid to late exponential phase (A_{600} 1.5 to 3), and cells were separated from supernatants by centrifugation (16,000 × *g*, 15 min, 4 °C).

Supernatants were concentrated by lyophilization, redissolved in 1 ml of deuterated methanol (Sigma) and used for the identification of extracellular by-products. ^{13}C nuclear magnetic resonance (^{13}C NMR) spectra were recorded on a Brucker AV200 spectrometer at 200 MHz and 25 °C, with a relaxation time of 1.5 s. Signals for pyruvate, gluconate, and acetate were assigned by comparison with previously published chemical shifts (Spectral Database for Organic Compounds) and confirmed by comparison with ^{13}C NMR spectra of pure compounds.

Compatible solutes (ectoines, glutamate, and trehalose) and membrane lipids were extracted from the cell pellets by a variation of the protocol described by García-Estepa *et al.* (12). The aqueous phase was used for the analysis of compatible solutes, and the chloroform phase for membrane lipids. Spectra were recorded at 25 °C using Brucker AV400 and Brucker AV600 spectrometers at 400 and 600 MHz, respectively, and a relaxation time of 3 s. Peak areas were integrated for relative quantification.

Spectrophotometric Determination of Glucose and Ammonia Consumption—Glucose was assayed by a glucose (hexokinase) assay kit (GAHK20, Sigma). Ammonium was assayed by an enzymatic assay kit (11112732035, from R-Biopharm, Darmstadt, Germany). Kits were used according to the recommendations of the manufacturers. Measurements were performed in a 96-well microplate reader Synergy HT (Bio-Tek, Winooski, VT).

Enzyme Assays

Enzyme assays were optimized for the conditions, media, and the microorganisms used in this work. Measurements were carried out in a 96-well microplate reader Synergy HT (Bio-Tek, Winooski, VT). A unit of enzyme activity was defined as micromoles of substrate consumed or product formed per min and was normalized to milligrams of protein (units·mg^{-1}).

In each case, reactor bulk samples were withdrawn, and cells were centrifuged (16,000 × *g*, 15 min, 4 °C) and resuspended in 65 mM phosphate buffer (pH 7.5). Cells were sonicated on ice with a 3-mm diameter probe using a Vibra Cell VC 375 ultrasonic processor (Sonics Materials, Danbury, CT) and centrifuged (16,000 × *g*, 20 min, 4 °C). The supernatant (cell-free extract) was used for subsequent activity measurements. Protein concentration in cell-free extracts was determined by the bicinchoninic acid (BCA) method (BCA Protein Assay kit, Pierce).

The protocols for the assessment of the activity of 6-phosphofructokinase (Pfk) (21), glucose-6-phosphate dehydrogenase (21), citrate synthase (Cs) (21), $NADP^+$/NAD^+-dependent isocitrate dehydrogenase (Icdh) (22), pyruvate carboxylase (Pc) (23), phosphoenolpyruvate carboxylase (Ppc) (23), isocitrate lyase (22), malic enzyme (24), aspartate aminotransferase (25), NADPH and NADH-dependent glutamate dehydrogenase (Gdh) (26) were optimized for *C. salexigens* (see supplemental material).

In Silico Analysis of Protein Homology

The completely sequenced and annotated genome of *C. salexigens* is available on line. However, the annotations have been made by automated homology studies of ORFs from many microorganisms, and there may be some incorrect assignments or gaps in the information. To analyze in detail the ORF assignments of the metabolic pathways more relevant for this work, we compared the metabolic reconstruction made by Ates *et al.* (18) with information available at genome sequence-based databases, such as the Kyoto Encyclopedia of Genes and Genomes (KEGG) (27), and MetaCyc (28), which are supported by experimental data. Gene and protein sequences were compared using BLAST (29). Analyses of domains (Conserved Domain Database, www.ncbi.nlm.nih.gov), protein localization and topology (Signal P 4.0 server), and genomic context were also performed.

Prediction of the Fates of Isotopic Labels

[1-^{13}C]-, [2-^{13}C]-, and [6-^{13}C]glucose were selected specifically for interrogating the relative importance of different pathways of central metabolism, as described previously (30, 31). The patterns of incorporation of the isotopic label from glucose into pyruvate and acetyl-CoA via glycolysis or the Entner-Doudoroff pathway and then into ectoines were predicted.

RESULTS

High Salinity Favors Biomass and Ectoine Production by C. salexigens

To study the effect of salinity on the metabolism of *C. salexigens*, the production of biomass and ectoines was determined in cultures grown with glucose as the sole carbon source at 0.6, 0.75, 2.5, and 3 M NaCl. Maximum biomass production increased with salinity up to 2.5 M NaCl (Table 1), whereas

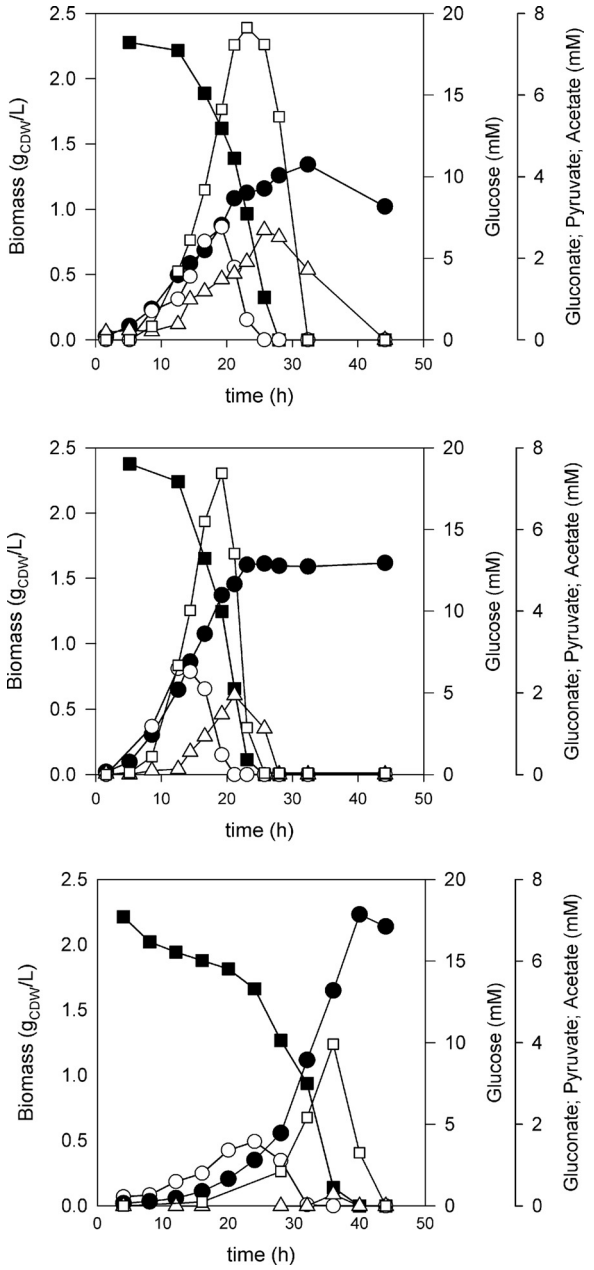

FIGURE 1. **Formation of biomass (*black circles*) and extracellular concentrations of glucose (*black squares*), gluconate (*white circles*), pyruvate (*white squares*), and acetate (*white triangles*) of batch cultures grown in 20 mM glucose minimal medium with 0.6 M NaCl (*A*), 0.75 M NaCl (*B*), and 2.5 M NaCl (*C*).**

growth rate was optimal in minimal medium M63 with 0.75 M NaCl (Fig. 1) (9, 12).

We reported previously that the intracellular content of ectoines increases with salinity (12), in agreement with the role of ectoines in osmoprotection. The stoichiometric coefficients of ectoines synthesis from biomass ($Y_{Ect/X}$) showed that total ectoines content was directly proportional to salinity (Table 1 and Fig. 2*A*). However, ectoines production rate was maximal at 2.5 M NaCl (Table 1). The hydroxyectoine to ectoine ratio increased with salinity up to 2.5 M NaCl (Table 1 and Fig. 2*A*), and an inverse correlation was observed between the relative content of ectoines and proteins with increasing salt concentration (Fig. 2*B*).

Consumption of Carbon and Nitrogen Sources

As the biosynthesis of ectoines occurs at the expense of central metabolic intermediates, it is expected to significantly burden metabolism. To assess salinity-dependent metabolic changes, nutrients and by-products were monitored at different salinities.

Glucose is the favorite carbon source for *C. salexigens* (32). The stoichiometric coefficient of glucose consumption was highly affected by salinity, being highest at 0.6 M NaCl and decreasing by 75% at 3 M NaCl (Fig. 2*C*). Ammonium consumption was quite different, because the stoichiometric coefficient of ammonium uptake remained practically unaltered regardless of salinity (Fig. 2*C*). This is a remarkable finding, because, in principle, the high production of ectoines at high salinity should lead to a higher demand of the nitrogen source. To better understand the overall alterations of metabolism at different salinities, we calculated the ammonium to glucose consumption molar ratio. This parameter increased with salinity up to 2.5 M NaCl (Fig. 2*C*), and a positive correlation between the specific ectoines production rate, and the ammonium to glucose consumption ratios was observed (Fig. 2, *A* and *B*).

Overall, our findings show that the slow down in growth and metabolism at high salt concentrations favor biomass production, which is in agreement with the previously observed effect of salt concentrations above 1.5 M NaCl (32). This underscores that the higher efficiencies of carbon and nitrogen metabolism at high salinity are the consequences of the specialization to cope with a highly demanding environment.

Quantification of Organic Acids Excreted by C. salexigens, Overflow Metabolism

The presence of gluconate, acetate, pyruvate, and minor amounts of lactate in supernatants of cultures grown at 0.6 and 0.75 M NaCl suggested a possible overflow metabolism. The consumption of glucose and ammonium and production and reutilization of organic acids were determined at three different salinities. At any salt concentration, glucose was the growth-limiting nutrient, because its depletion marked the entrance into stationary phase. In contrast, around 15 mM ammonium was still present in the medium at the end of growth of each culture (data not shown). At 0.6 and 0.75 M NaCl, acetate was produced during the exponential phase of growth (Fig. 1, *A* and *B*), although at high salinity (2.5 M NaCl) extracellular acetate was almost undetectable (Fig. 1*C*). The specific rate of production of pyruvate production during exponential growth decreased with salt concentrations (Table 2). Acetate and pyruvate were re-assimilated once glucose was totally depleted, in contrast with gluconate, which accumulated in the culture medium during early exponential phase of growth and was consumed along with glucose in the mid-to-late exponential phase (Fig. 1). As described in Table 2, gluconate, pyruvate, and acetate were the major excreted products. Production rates of the two latter conditions inversely correlated to the salt concentration and the biomass yield. These findings suggest an increased metabolic efficiency at high salinity.

The presence of these compounds in cultures grown suggested a possible overflow metabolism at low salinity. This

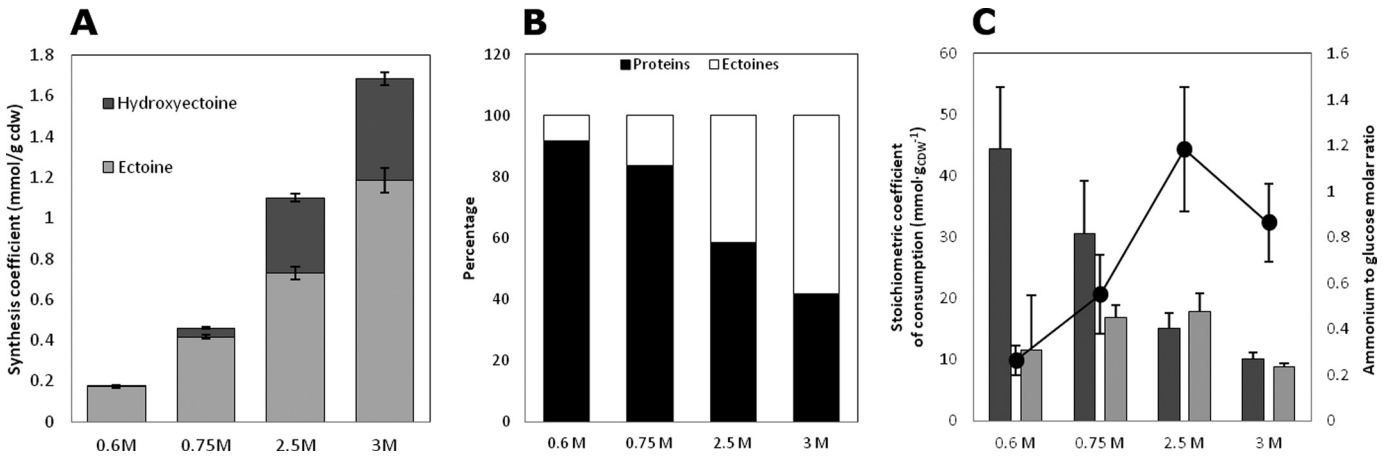

FIGURE 2. **Effect of NaCl concentration on production of ectoines and consumption of carbon and nitrogen sources in *C. salexigens*.** *A,* cellular contents of ectoine and hydroxyectoine. *B,* relative content of proteins and ectoines, expressed as percentage of total pool of ectoines plus proteins. The sum of these pools was approximately constant throughout all conditions tested (0.423 ± 0.055 g/g$_{CDW}$). *C,* stoichiometric coefficient of glucose (*dark bars*) and ammonium consumption (*light bars*). Molar ratio of ammonium to glucose utilization is denoted by *circles*. Cultures were grown at 37 °C in M63 minimal medium with 20 mM glucose and 30 mM ammonium as the sole carbon and nitrogen sources, respectively. See the text for details.

TABLE 2

Specific consumption/production rates of the main extracellular metabolites

Cultures were grown in glucose/M63 minimal medium. See under "Materials and Methods" for details. All rates were calculated in the early exponential phase of growth and (except for lactate production) are expressed in mmol·g$_{CDW}^{-1}$·h^{-1}.

[NaCl]	Glucose	Ammonium	Gluconate	Pyruvate	Lactate[a]	Acetate
$_{M}$						
0.6	14.28 ± 1.28	3.73 ± 2.87	0.87 ± 0.31	2.25 ± 1.20	0.00 ± 0.00	0.43 ± 0.17
0.75	11.73 ± 3.24	6.46 ± 0.75	1.14 ± 0.38	1.66 ± 0.51	13.2 ± 9.5	0.53 ± 0.20
2.5	2.1 ± 0.18	2.48 ± 0.40	0.97 ± 0.47	0.30 ± 0.17	0.00 ± 0.00	0.02 ± 0.01

[a] Lactate production rates are in μmol·g$_{CDW}^{-1}$·h^{-1}.

could arise from a limited catabolism of glucose, leading to a higher excretion of by-products due to the reduced demand for ectoines.

In Silico and in Vitro Analyses of Metabolic Pathways Related to the Synthesis of Precursors of Ectoines

In Silico Analysis

Accumulation of compatible solutes at high salinity imposes a biosynthetic burden on cells. The above results reflect that osmoadaptation in *C. salexigens* has implications on metabolic performance. *C. salexigens* genome has been automatically annotated, and preliminary analyses (16, 19) and a first genome-based metabolic reconstruction (18) have been published. To further understand the interplay between osmoadaptation and metabolism, we critically assessed a number of routes in this metabolic network related to central metabolism, with emphasis on the pathways leading to precursors of ectoines, as well as to metabolites found in supernatants. For this purpose, we performed the following: (i) homology studies using the information of related microorganisms such as Pseudomonads, Enterobacteria, and halotolerant bacteria available in metabolic databases such as MetaCyc and KEGG (27, 28); (ii) analysis of conserved domains, protein localization, and genomic context; (iii) growth experiments with D-glucono-1,5-lactone, D-gluconate, and 2-keto-D-gluconate as carbon sources, and (iv) review of literature data.

Genome analysis revealed interesting metabolic features. The ED pathway, which is a route for the catabolism of glucose to pyruvate (33), could be operative in *C. salexigens* (supplemental Fig. S1). Typically, microorganisms using the ED pathway lack glycolytic enzyme(s), such as Pfk (34, 35). In fact, unambiguous annotation of the gene encoding Pfk in *C. salexigens* has been difficult (19). There are five ORFs annotated in the JGI website (genome.ornl.gov) as potential phosphofructokinases, although they have low homology with *bona fide* Pfks (supplemental Fig. S2 and supplemental Table S1). There is also a putative pyrophosphate-dependent phosphofructokinase (Csal1534). The reaction catalyzed by this enzyme is readily reversible (36). However, the gene for this enzyme from *Propionibacterium freudenreichii* can only complement fructose-1,6-bisphosphatase (*fbp*) mutations but not phosphofructokinase (*pfkA/pfkB*) mutations in *Escherichia coli* (37), indicating that it functions in the gluconeogenic direction but not in the glycolytic direction. Significantly, the analysis of the *C. salexigens* genome also failed to identify a clear-cut representative of a fructose bisphosphatase (19), raising the possibility that Csal1534, which has been annotated as Ppi-Pfk, may be a fructose bisphosphatase.

Our *in silico* analysis suggests that oxidation of D-glucose to D-gluconate through D-glucono-1,5-lactone could occur both in the periplasm and the cytoplasm. This agrees with our finding of the early accumulation of D-gluconate in the growth medium. *C. salexigens* was able to grow with D-glucono-1,5-lactone, D-gluconate, and 2-keto-D-gluconate as the sole carbon source (supplemental Fig. S4), and a variant of the 2-keto-gluconate loop described in *Pseudomonas* (38) was predicted to be functional in *C. salexigens* (Fig. 3 and supplemental Fig. S1).

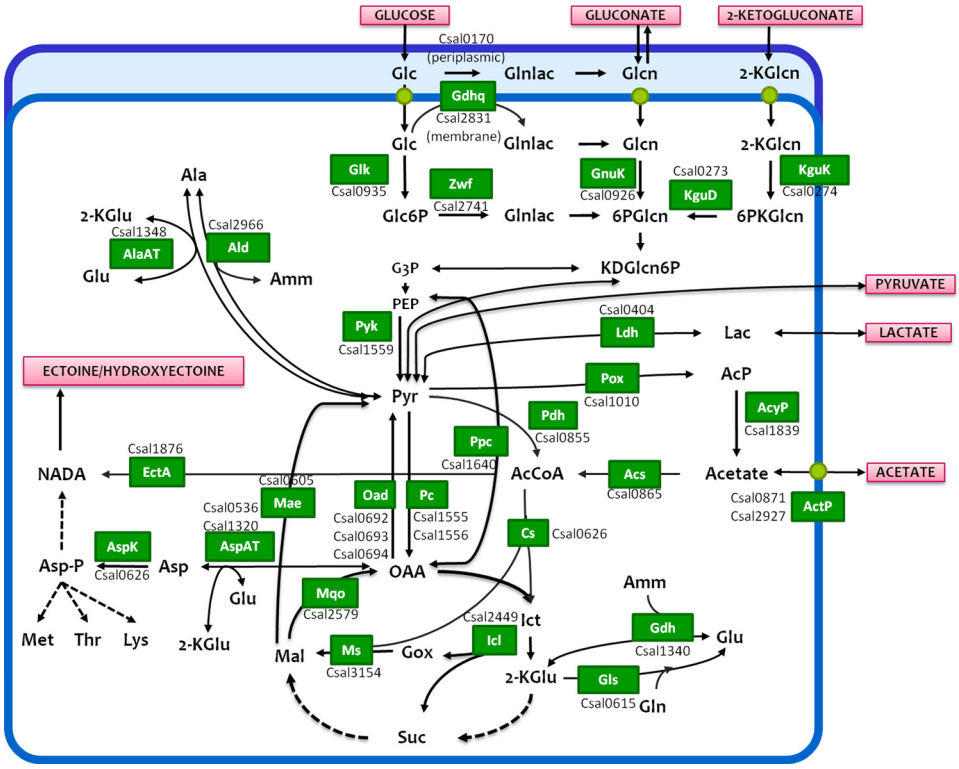

FIGURE 3. **Scheme of the central metabolism and synthesis of ectoines in *C. salexigens* based on the annotated genome.** Pathways leading from glucose to 6-P-gluconate (*6PGln*) are proposed on the comparison of the *in silico* analysis of *C. salexigens* and *P. putida.* Abbreviations used are as follows: *2-KGlcn*, 2-ketogluconate; *2-Kglu*, 2-ketoglutarate; *6PGlcn*, 6-phospho-D-gluconate; *6PKGlcn*, 6-phospho-2-keto-D-gluconate; *AcCoA,* acetyl-coenzyme A; *AcP*, acetyl phosphate; *Ala*, L-alanine; *Amm*, ammonium; *Asp*, L-aspartate; *Asp-P*, L-aspartyl phosphate; *G3P*, glyceraldehyde 3-phosphate; *Glc*, D- glucose; *Glc6P*, D-glucose 6-phosphate; *Glcn*, D-gluconate; *Glcnlac*, D-gluconolactone; *Gln*, L-glutamine; *Gox*, glyoxylate; *Glu*, L-glutamate; *Ict*, D-isocitrate; *KDGlcn6P*, 2-keto-3-deoxy-D-gluconate-6-phosphate; *Lac*, D-lactate; *Lys*, L- lysine; *Mal,* L-malate; *Met*, L-methionine; *NADA, N*-γ-acetyl-L-2,4-diaminobutyrate; *OAA*, oxaloacetate; *PEP*, phosphoenolpyruvate; *Pyr*, pyruvate; *Suc*, succinate; *Thr,* L-threonine; *Acs*, acetyl-coenzyme A synthetase; *ActP*, acetate permease; *AcyP*, acetyl phosphate phosphatase; *AlaAT*, alanine aminotransferase; *Ald,* alanine dehydrogenase; *AspAT*, aspartate aminotransferase; *AspK*, aspartate kinase; *Cs*, citrate synthase; *EctA*, diaminobutyrate acetyltransferase; *Gad*, gluconate dehydrogenase; *Gdhq*, glucose dehydrogenase; *Gdh*, glutamate dehydrogenase; *Glk*, glucokinase; *Gls*, glutamate synthase; *GnuK*, gluconokinase; *Icl*, isocitrate lyase; *KguD,* 2-keto-6-phosphogluconate reductase; *KguK*, 2-ketogluconate kinase; *Ldh*, lactate dehydrogenase; *Mae*, malic enzyme; *Mqo*, malate-quinone oxidorreductase; *Ms*, malate synthase; *Oad*, oxaloacetate decarboxylase; *Pc*, pyruvate carboxylase; *Pdh*, pyruvate dehydrogenase; *Pox,* pyruvate oxidase; *Ppc*, phosphoenolpyruvate carboxylase; *Pyk,* pyruvate kinase; *Zwf,* glucose-6-phosphate dehydrogenase. *Dashed arrows* are used for conversions that require more than one enzymatic step.

C. salexigens possesses genes specifying putative Pc, Ppc, and OAA decarboxylase (supplemental Table S1). These enzymes interconvert pyruvate, phosphoenolpyruvate, and OAA and could have a role in supporting high ectoine biosynthetic fluxes by replenishing OAA needed for the TCA cycle (Fig. 3).

The observed production of acetate is difficult to explain in the light of the current genome annotation and knowledge of metabolic pathways. Acetate metabolism in *C. salexigens* is quite different from that of *Pseudomonas* and *E. coli*. The main route of acetate production in *P. aeruginosa, E. coli,* and related species is the phosphotransacetylase acetate kinase pathway (39), which is not present in *C. salexigens*. Acetate production in the latter bacterium could involve the formation of the high energy intermediate acetyl phosphate through an alternative route. Csal1010 is annotated as a soluble pyruvate oxidase. This FAD-dependent enzyme decarboxylates pyruvate, producing acetate (28). The catabolism of ectoines also yields acetate (40); in fact, continuous synthesis and degradation of ectoines at low salinity could explain the higher acetate overflow.

Regarding nitrogen metabolism, there is one copy of genes for alanine aminotransferase, L-alanine dehydrogenase, glutamate synthase, and glutamate dehydrogenase in the *C. salexigens* genome. The enzymes specified by these genes are responsible for reductive transfer of ammonium to 2-ketoglutarate to generate glutamate (41, 42), which acts as the major ammonium donor in the cell. There are two putative aspartate aminotransferases, which catalyze the reversible transfer of the amino group from glutamate to oxaloacetate, rendering aspartate and 2-ketoglutarate. This is a key enzyme as it links the TCA cycle with the first enzyme of the ectoines synthesis pathway (aspartokinase). *C. salexigens* has only one aspartokinase catalyzing the formation of aspartyl phosphate, which is a common metabolic intermediate in the biosynthesis of ectoines and aspartate family of amino acids (8, 19). For a complete description of the *in silico* analysis, see supplemental Table S1 and Figs. S1–S4.

In Vitro Analysis

Activities of selected enzymes were determined *in vitro*. The enzymes assayed belonged to four main groups as follows: (i) glucose/gluconate metabolism; (ii) TCA cycle; (iii) anaplerotic and gluconeogenic reactions, and (iv) nitrogen metabolism. Enzyme activities were determined in the mid-exponential phase cultures at different salinities (Table 3).

TABLE 3

Enzyme activities in crude extracts of exponential phase of batch cultures grown in glucose/M63 containing 0.6, 0.75, and 2.5 M NaCl

All values are given in milliunits·(mg protein)$^{-1}$. Data are the averages of eight determinations (four independent cultures, assayed in duplicate). NM means not measured. Zwf is glucose-6-phosphate dehydrogenase; Icl, isocitrate lyase; Mae, malic enzyme; AspAT, aspartate aminotransferase.

Enzyme activity	NaCl concentration		
	0.6 M	0.75 M	2.5 M
Gluconate metabolism			
Zwf	39.1 ± 15.5	55.7 ± 27.4	48.8 ± 16.5
Glycolysis and TCA cycle enzymes			
Pfk	NM	<0.05	<0.05
Cs	32.5 ± 22.3	71.7 ± 38.7	66.5 ± 40.9
Icdh	462 ± 189	645 ± 295	554 ± 183
Anaplerotic pathway enzymes			
Icl	1.27 ± 0.69	2.30 ± 1.24	1.93 ± 0.70
Mae	5.69 ± 2.86	7.99 ± 6.83	5.87 ± 2.18
Pc	92.2 ± 19.1	70.6 ± 8.2	167.0 ± 28.0
Ppc	NM	9.02 ± 3.67	15.82 ± 4.42
Nitrogen metabolic enzymes			
NADPH-Gdh	22.3 ± 7.60	73.7 ± 31.4	16.4 ± 9.0
NADH-Gdh	52.5 ± 36.0	71.1 ± 46.4	74.1 ± 51.3
AspAT	95.2 ± 18.0	174 ± 93	78.5 ± 16.5

Glucose Metabolic Enzymes, Glucose-6-phosphate Dehydrogenase and Pfk—Glucose-6-phosphate dehydrogenase interconnects the EM, ED, and pentose phosphate pathways (43) and is considered as a major route for NADPH production for biosynthesis and redox homeostasis (Table 3).

Significantly, we were unable to detect Pfk activity above background in cell-free extracts (Table 3 and supplemental Tables S1 and S2 and Figs. S1–S3). This fact along with the lack of unequivocal assignment for Pfk suggests that, like Pseudomonads and some other aerobic genera (44), *C. salexigens* uses the ED pathway for glucose catabolism, whereas the operation of functional glycolysis remains uncertain (Fig. 3).

TCA Cycle Enzymes, Cs and Icdh—In addition to their important role for the supply of metabolic energy, TCA cycle intermediates are key building blocks for the synthesis of biomass and ectoines (Fig. 3). Two activities of the TCA cycle were determined, Cs and Icdh. Two Icdh-encoding genes are annotated (Csal0525 and Csal1434), which differ in cofactor specificity; however, only $NADP^+$-dependent Icdh activity was detected. Regardless of salinity, Icdh activity was 8–15-fold higher than that of Cs (Table 3).

Anabolic and Anaplerotic Pathways Enzymes, Ppc, Pc, Isocitrate Lyase, and Malic Enzyme—Anaplerotic pathways are essential to replenish the OAA in the TCA cycle that is withdrawn for the production of ectoines (Fig. 3). Both Ppc and Pc activities were detected, the latter being 8–10-fold higher than the former. Interestingly, the Pc and Ppc activities measured in cells grown at 2.5 M NaCl were 2-fold higher than observed at low salinities (Table 3).

The activity of the anaplerotic enzymes isocitrate lyase (isocitrate lyase and glyoxylate shunt) and malic enzyme (malic enzyme, gluconeogenesis) (45) was low compared with other activities analyzed. This is in agreement with what has been described in glucose-grown *E. coli* and *Pseudomonas aeruginosa* (46, 47).

Nitrogen Metabolism Enzymes, Aspartate Aminotransferase and Glutamate Dehydrogenase—Glutamate dehydrogenase (Gdh) along with glutamine synthetase and glutamate synthase are the routes of ammonium assimilation in bacteria. Both NADH- and NADPH-dependent Gdh activities were detected in *C. salexigens* extracts. Only the NADH-Gdh enzyme was predicted from the genomic sequence of *C. salexigens* (Csal1340) suggesting that it may not discriminate between the two pyridine nucleotides. Transaminases, catalyzing the transfer of the amino group between amino acids, are involved in amino acid synthesis. Aspartate aminotransferase activity was high, which should not be surprising considering that this activity must account for the synthesis of ectoines and all amino acids from the aspartate family (Fig. 3).

Enzyme Activities and in Vivo Fluxes—Enzyme activities determined *in vitro* can be viewed as estimates of flux through a given route. Intracellular carbon fluxes can be roughly estimated from glucose uptake rates. When compared with Cs and Pc activities, the following is evident: (i) Cs activity was similar at all three salt concentrations, whereas Pc activity was higher at 2.5 M NaCl (Table 3), and (ii) the glucose uptake rate was 5–30-fold higher than Cs and Pc activities (the difference being higher at low salinity, supplemental Table S3). Although this is a rough approximation, these facts are in accord with our data on the accumulation of extracellular metabolites (Table 2) explaining why cells divert a significant part of the metabolized glucose to pyruvate and acetate overflow and suggesting that the TCA cycle might be limited by the low Cs activity. In addition, the high Pc activity indicated that OAA was actively synthesized from pyruvate.

Tracing Ectoines Labeling from Glucose

Finally, to assess the distribution of fluxes of central metabolism, the biosynthetic pathways for ectoines production were traced by isotopic labeling with [1-^{13}C]-, [6-^{13}C]-, and [2-^{13}C]glucose at low and high salinity. All possible isotopomers derived from these precursors via the EM and ED pathways, anaplerosis and the TCA cycle, were predicted for pyruvate, PEP, OAA, acetyl-CoA, and ectoines, based on the annotated genome (supplemental Fig. S5 and Tables S3 and S4).

Ectoines Labeling in [1-^{13}C]- and [6-^{13}C]Glucose-grown Cultures—The analysis of the labeling of ectoines with [1-^{13}C]- and [6-^{13}C]glucose provides a way to estimate the EM to ED flux ratio. In cells grown with [1-^{13}C]glucose, the COOH and C6 of ectoines were predominantly labeled, regardless of the salt concentration, and the labeling of the other carbons was close to the natural abundance of the ^{13}C isotope (Fig. 4). The labeling of COOH can be explained by use of the ED pathway. Surprisingly, C6 of ectoines contained substantially higher amount of ^{13}C than would be predicted from natural abundance. We can account for this excess labeling of C6 of ectoines by postulating that $^{13}CO_2$ generated by decarboxylation of [1-^{13}C]pyruvate is reincorporated efficiently by the carboxylation of either Pc or Ppc. The enrichment of label at the COOH of ectoines allowed us to estimate that over 95% of glucose used for ectoines synthesis was metabolized through the ED pathway and Pc. Label scrambling due to other pathways such as the pentose phosphate pathways could explain minor label enrichment at other positions. Also, the existence of a functional but minor glycolysis cannot be firmly dismissed.

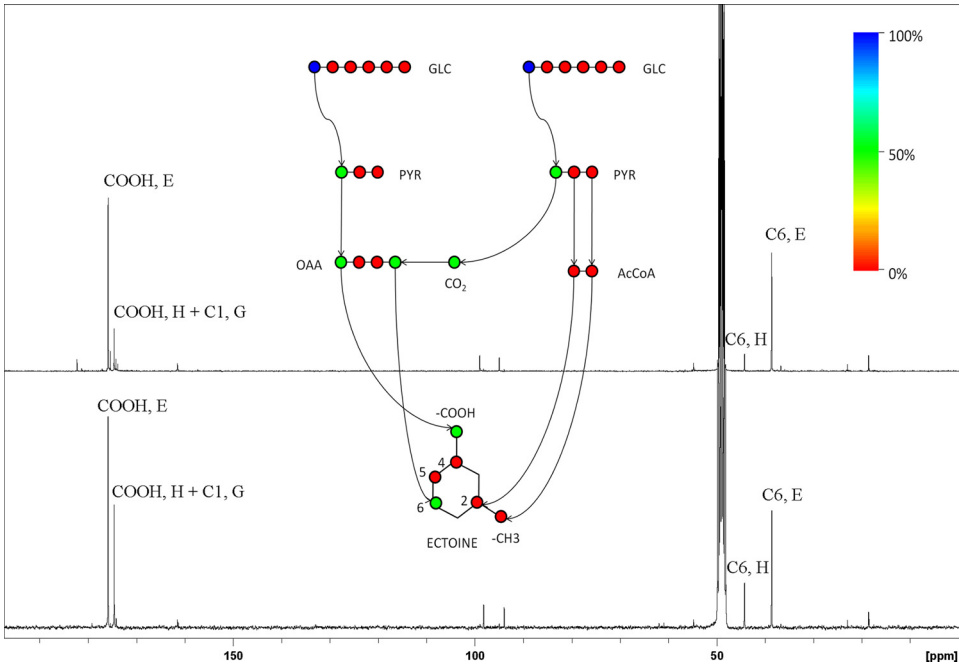

FIGURE 4. **^{13}C NMR spectra of intracellular extracts of [1-^{13}C]glucose-grown cultures.** M63 minimal medium with 0.75 M NaCl (*upper spectrum*) and 2.5 M NaCl (*lower spectrum*) was used. The signals corresponding to labeled carboxylic carbon (177 ppm for ectoine and 174–175 for hydroxyectoine) and C6 (38–39 ppm for ectoine and 44 for hydroxyectoine) are shown. In the scheme, the expected fate of labeled carbon when [1-^{13}C]glucose is metabolized via the Entner-Doudoroff pathway is shown. If we assume that the labeled C1 from pyruvate is lost as $^{13}CO_2$ by decarboxylation at the level of Pdh and incorporated into OAA by Pc, the predicted ectoines labeling pattern would fit the spectra obtained. Relative labeling for each carbon atom is indicated by the *color scale* at *right*. The abbreviations used are as follows: labeled compounds detected: *G,* glutamate; *E,* ectoine; *H,* hydroxyectoine; *GLC,* glucose; *PYR,* pyruvate; *OAA,* oxaloacetate; *AcCoA,* acetyl-coenzyme A.

The results obtained with [6-^{13}C]glucose, which were complementary to those obtained with [1-^{13}C]glucose, demonstrated that the incorporation of label into ectoines from C1 and C6 of glucose is not equivalent (supplemental Fig. S6). This result shows that glucose catabolism occurs through asymmetrically labeled 3-carbon metabolites, contrary to what would be predicted for the EM pathway. In addition, the more efficient incorporation of ^{13}C label into the glycerol moiety of membrane phospholipids from [6-^{13}C]glucose than from [1-^{13}C]glucose (supplemental Figs. S7 and S8) is also in accord with the labeling of ectoines. Thus, these data demonstrate that *C. salexigens* metabolizes glucose through the ED pathway and, together with the uncertainty of the existence of Pfk, suggest that the EM pathway is not functional.

Ectoine Labeling in [2-^{13}C]Glucose-grown Cultures—For [2-^{13}C]glucose as carbon source, metabolism via the EM pathway would be predicted to yield PEP and pyruvate that are both 50% labeled in their C2. Metabolism via the ED pathway would also generate [2-^{13}C]pyruvate but would not produce any [^{13}C]PEP (supplemental Fig. S5). Therefore, the metabolic fate of the [2-^{13}C]pyruvate pool can be analyzed without any further assumptions (Fig. 5). OAA could be synthesized from pyruvate/PEP in *C. salexigens* by the following routes: (i) carbons from pyruvate can enter the TCA cycle as acetyl-CoA produced by Pdh, rendering OAA after one turn of the cycle (Fig. 5*A*); (ii) pyruvate and PEP can be carboxylated to OAA by Pc or Ppc (Fig. 5*B*), or (iii) by a combination of both routes (Fig. 5*C*). From the spectra of ectoines, we can conclude that the contribution of Ppc to the total anaplerotic activity of the cells is negligible (supplemental material). This would be in agreement with the measured enzyme activities (Table 3).

Labeling of C6 and the carboxylic group of ectoines increase as a function of the Pdh flux, whereas labeling of C4 depends on the Pc flux. The labeling of C2 of ectoines is the result of the incorporation by EctA of the Pdh-produced acetyl-CoA. None of the pathway combinations would yield ectoines labeled at the methyl group. These predictions fit well with the corresponding spectra, where the signal coming from the methyl group is the least intense and the most intense signals were those of C2 and C4 (Fig. 5*E*).

Effect of Salinity on Metabolic Fluxes, the Pc/Pdh, Cs/EctA, and Pc/Cs Flux Ratios

To understand the functioning of central metabolic pathways in *C. salexigens*, the partitioning of pyruvate and acetyl-CoA can be described by the Pc/Pdh and Cs/EctA ratios. The Cs/EctA flux ratio describes the fraction of acetyl-CoA that enters the TCA cycle *versus* the fraction that is directly incorporated into ectoines. The Pc/Pdh flux ratio indicates the fraction of pyruvate that is transformed to OAA *versus* oxidized to acetyl-CoA. Finally, the Pc/Cs ratio allows comparison of the activity of anaplerosis and the TCA cycle and can be considered as readout of the biosynthetic or energetic needs of the cells (Fig. 3).

The ^{13}C-labeling pattern of ectoines synthesized from [2-^{13}C]glucose can be used to quantify relative fluxes at these nodes (Table 4). For that aim, the metabolic steady state hypothesis was considered applicable to exponential cultures (and therefore labeling at the specific positions of the ectoine molecule is proportional to fluxes). Peak areas in ^{13}C NMR spectra were used to estimate flux ratios, using simple algebraic equations (supplemental material). The ^{13}C NMR spectra of

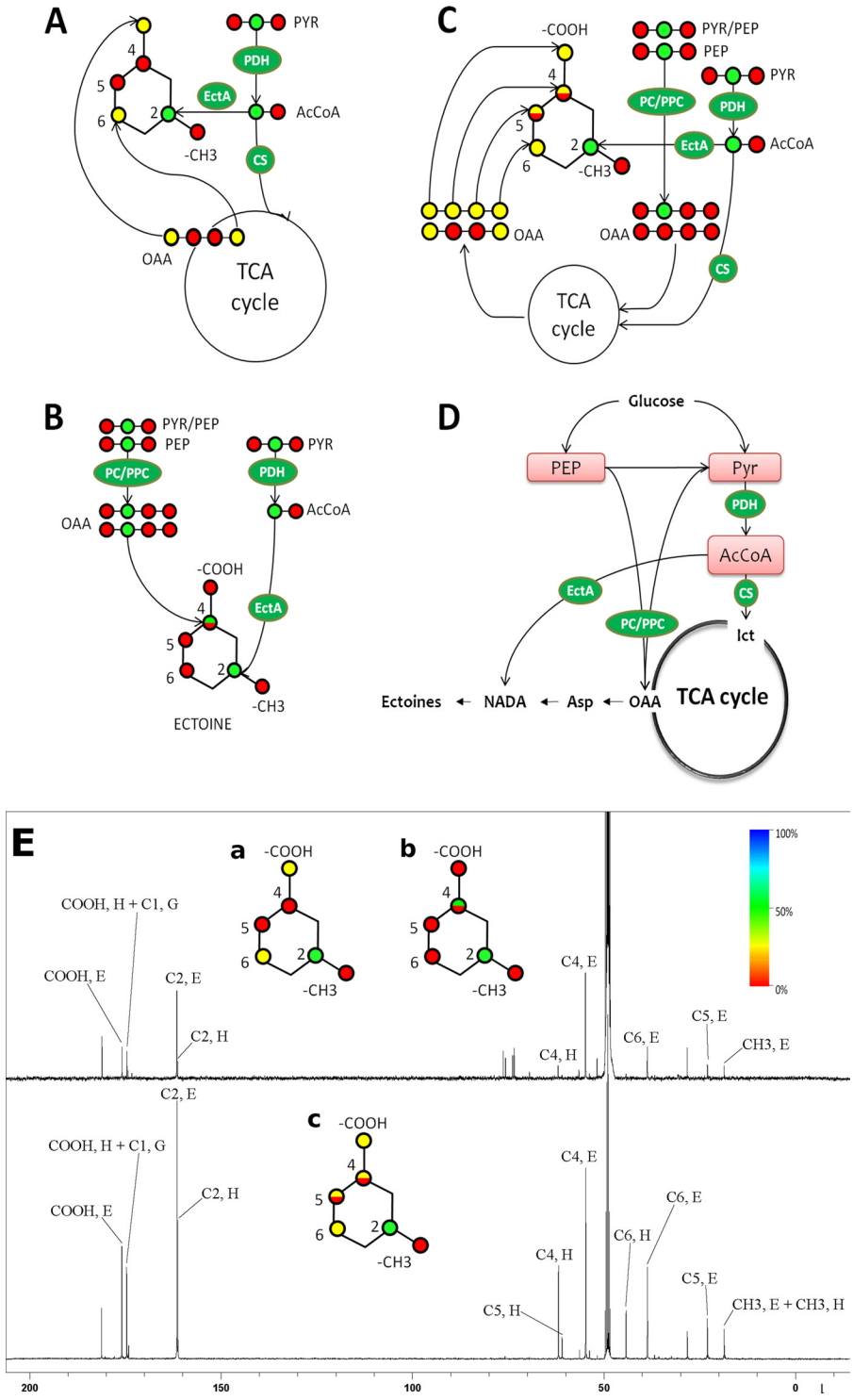

FIGURE 5. **Incorporation of label from [2-^{13}C]glucose into ectoines.** ^{13}C from [2-^{13}C]pyruvate (derived via either the Embden-Meyerhof or the Entner-Doudoroff pathways), from [2-^{13}C]phosphoenolpyruvate (made via Embden-Meyerhof), or from unlabeled phosphoenolpyruvate (made via Entner-Doudoroff) can be incorporated into ectoines through the following. *A,* oxaloacetate synthesized in a single TCA cycle turn; *B,* oxaloacetate synthesized by pyruvate carboxylase or phosphoenolpyruvate carboxylase (*Pc/Ppc*), or (*C*) oxaloacetate synthesized by Pc/Ppc followed by a turn through the TCA cycle, which alters its labeling pattern (see the text for details). *D,* scheme depicting the relation of the pyruvate and acetyl-CoA nodes with the ectoines biosynthesis route in *C. salexigens*. *E,* ^{13}C NMR spectra from intracellular extracts of [2-^{13}C]glucose-grown cultures. M63 minimal medium with 0.75 M NaCl (*upper spectrum*) and 2.5 M NaCl (*lower spectrum*) was used. The signal corresponding to labeled carboxyl carbon, methyl carbon, C2, C4, and C6 of ectoine (*E*) and hydroxyectoine (*H*) are shown. The signal corresponding to hydroxyectoine carboxyl carbon overlaps with that of C1 of glutamate (indicated as C1, *G*). Note that for each pair of chemical shifts corresponding to each carbon, the ratio of the ectoine/hydroxyectoine signals is approximately constant. The three ectoine molecules in the *inset* represent the isotopomer distributions corresponding to *a–c*. Relative labeling for each carbon atom is indicated by the *color scale* at *right* of *E*. Where applicable, the upper half of the corresponding carbon position ball depicts the expected labeling from [2-^{13}C]pyruvate/[2-^{13}C]phosphoenolpyruvate, and the lower half from unlabeled phosphoenolpyruvate. See supplemental Table S4 and Fig. S5 and supplemental material "Determination of Metabolic Flux Ratios" for details.

TABLE 4

Metabolic flux ratios estimated from the ectoine and hydroxyectoine labeling patterns observed in ^{13}C NMR spectra from cultures in [2-^{13}C]glucose M63 minimal medium with 0.75 and 2.5 M NaCl

The abbreviations used are as follows: Pdh, pyruvate dehydrogenase; Pc, pyruvate carboxylase; EctA, diaminobutyrate acetyltransferase; Cs, citrate synthase.

Flux ratio	Ectoine (0.75 M NaCl)	Ectoine (2.5 M NaCl)	Hydroxyectoine[a] (2.5 M NaCl)
Pc/Pdh	0.67 ± 0.10	0.61 ± 0.13	0.55 ± 0.07
Cs/EctA	0.70 ± 0.03	0.71 ± 0.02	0.68 ± 0.04
Pc/Cs	1.64 ± 0.07	1.49 ± 0.33	1.37 ± 0.22

[a] The signal of the carboxyl group of hydroxyectoine overlaps with glutamate C1 signal. Integration areas of these signals were estimated.

intracellular ectoines point to a flux distribution where both anaplerosis and the TCA cycle noticeably contribute to carbon flux from pyruvate to ectoines. In fact, Pdh flux is almost twice as high as the Pc flux, and the Cs flux is lower than the EctA flux (Table 4). The Pc/Cs ratio revealed that the ratio of anaplerosis and catabolism is similar at the three salinities assayed. This is surprising, because a lower biosynthetic burden was expected at low salt concentration, when ectoine synthesis is low (Fig. 2*A*), and it might be related to overflow metabolism and the low activity of Cs (Table 3). Similar results were obtained regardless of using the ^{13}C NMR spectra of ectoine or hydroxyectoine (Table 4). In addition, the COOH signal from [1-^{13}C]glucose was almost twice as high as the C6 signal (Fig. 4), which is in accordance with the deduced Pc/Pdh flux ratio. Altogether, this indicates that acetyl-CoA used by EctA for ectoine synthesis is higher than that consumed in the TCA cycle even under conditions of low ectoine production, and it also explains the poor performance of *C. salexigens* at low salinity.

DISCUSSION

In this work we gained new insights into the central metabolism used by *C. salexigens*. To thrive in high saline environments, this halophile synthesizes ectoines as the main compatible solutes. The biosynthetic pathway of ectoines drains OAA and acetyl-CoA, which are central metabolic intermediaries. Therefore, adaptations developed by *C. salexigens* may also compromise its physiology, especially under low salt conditions.

In agreement with this, overflow metabolism and lower biomass yield were found at low salinity, coinciding with the low production of ectoines. Tracing labels from [1-^{13}C]-, [6-^{13}C]-, and [2-^{13}C]glucose to ectoines allowed us to probe the routes used by *C. salexigens* for glucose catabolism and ectoine production. One of the major conclusions from our labeling studies is that *C. salexigens* uses the ED pathway for glucose catabolism instead of the EM glycolytic pathway. This conclusion is supported by the absence of a standard ATP-linked phosphofructokinase activity and by the patterns of incorporation of label from [1-^{13}C]- and [6-^{13}C]glucose into ectoines and glycerol 3-phosphate. In this regard, *C. salexigens* is similar to *Pseudomonas* species (23, 38, 48) and other microorganisms (34, 35, 49, 50) that use ED for the catabolism of hexoses. Our finding that *C. salexigens* lacks a complete glycolytic pathway underscores the need for a full understanding of the pathways that are actually used by organisms before meaningful theoretical models of metabolism, such as flux balance analysis, can be fruitfully constructed.

After initial extracellular accumulation, gluconate was consumed during the exponential phase along with glucose (Fig. 1). This behavior suggests that, as in *Pseudomonas putida* and *Klebsiella pneumoniae*, gluconate is produced at an early and fast step of glucose oxidation, and its assimilation is limited by subsequent slower reactions (38, 51). This may not be the only way of glucose incorporation into the ED pathway, because glucokinase and glucose-6-phosphate dehydrogenase are annotated in the *C. salexigens* genome (supplemental Table S1). The detection of glucose-6-phosphate dehydrogenase activity (Table 3) suggests that glucose could also enter the ED pathway by the conversion of glucose 6-phosphate to 6-phosphoglucono-1,5-lactone and gluconate 6-phosphate (Fig. 3). Additionally, *C. salexigens* is able to grow on D-glucono-1,5-lactone, D-gluconate, and 2-keto-D-gluconate as single carbon sources (supplemental Fig. S4). Thus, various carbon sources can feed the ED pathway, similar to what has been described in *P. putida* (supplemental Fig. S1) (38).

The ED pathway is used for glucose oxidation by numerous mesophilic and halophilic bacteria and archaea (2, 52, 53). In hyperthermophilic archaea, it has been proposed that the presence of nonphosphorylative and semi-phosphorylative variants of the ED pathway may play an important role for thermoadaptation, allowing cells to avoid the production of heat-labile intermediaries (54). Although it is not clear whether this pathway confers any advantage for adaptation to high salinity, considerations of the overall balance of the pathway may shed light on the reason for its preferential utilization. Although the EM pathway produces 2 ATP and 2 NADH per glucose, the ED pathway is characterized by a lower energy yield, producing only 1 ATP per glucose. Additionally, the redox balance of the ED pathway can be different, depending on whether glucose is oxidized in the cytoplasm by the phosphorylative pathway or in the periplasm by the nonphosphorylative route (Fig. 3). In the first case, 1 NADPH and 1 NADH are produced, and in the second case, only 1 NADH and a reduced quinone are formed. The lower biomass yield in the cultures using the more oxidized compound 2-keto-D-gluconate as carbon source (supplemental Fig. S4) might also point to the relevance of NADPH for efficient growth and production of ectoines. The synthesis of ectoines consumes 3 NADPH equivalents, and the pathways used for glucose metabolism must be able to provide not only the carbon skeleton but also the necessary reducing equivalents. The existence of alternate pathways for glucose metabolism differing in the redox balance may allow the microorganism to control the rate of production of redox equivalents and to finely tune its redox state to maximize growth and ectoines biosynthesis.

The analysis of the labeling of ectoines also permitted us to estimate flux partitioning between the TCA cycle and the anaplerotic pathways (Fig. 5). Pc was the major anaplerotic reaction. The Pc/Pdh flux ratio estimated from the ectoines labeling pattern ranged between 0.55 and 0.67 (Table 4), whereas in glucose cultures of mesophilic bacteria like *E. coli*, *Bacillus subtilis,* or *Corynebacterium glutamicum* this ratio does not exceed 0.4 (47, 55, 56). Although this may not seem to be a large difference, we have to bear in mind that more than half of the acetyl-CoA produced by Pdh is consumed by EctA,

which, under high salinity represents a substantial amount. In fact, the high Pc activity combined with the Pc/Cs flux ratio better reflects a high anaplerotic flux (Table 4) and indicates that anaplerosis plays an important role in replenishing the OAA that is withdrawn for ectoines synthesis.

The enzyme activities we obtained are in agreement with those reported in other bacteria such as *P. aeruginosa* (48) or *E. coli* (21, 39). Consistent with the high need for anaplerosis, the Pc activity was higher than that observed in mesophilic bacteria (48). Furthermore, the estimated flux ratios, the measured activities of most enzymes, and the ammonium consumption coefficients were kept almost constant at different salinities, regardless of the different requirements for the synthesis of ectoines. Remarkably, enhanced production of ectoines at high salinities occurred at the expense of lower protein production (Fig. 2*B*), balancing the total ammonium consumption (57). Altogether, this gives an idea of a certain metabolic rigidity which, together with the high glucose uptake rate and the high Pc/Cs ratio, is the basis for the lower efficiency and metabolic overflow at low salt concentrations. The high glucose uptake rates at low salinity are in accordance with what has been described for acetate overflow in *E. coli* (58). Because the Cs/EctA ratios at low and high salinities are similar, this indicates that incorporation of acetyl-CoA to the TCA cycle is limiting at low salinity.

Our result that the metabolic efficiency of *C. salexigens* is higher at high salinity is surprising and seems to be counterintuitive, because as has been argued by Oren (4), the synthesis of high concentrations of organic compatible solutes that are needed for osmotic balancing could be predicted to impose a large burden on the carbon and energy budget of the cells. It should be borne in mind that overflow metabolism was observed under laboratory conditions using a relatively high concentration (20 mM) of glucose as a sole carbon source, and therefore it may not be representative of the metabolism by *C. salexigens* in its natural environment. Interestingly, the metabolites excreted by *C. salexigens* during exponential growth were scavenged to be used as secondary carbon sources at later times of cultures. Although glucose and gluconate were preferentially and simultaneously used, consumption of other organic acids did not start until glucose was exhausted, indicating that catabolite repression mechanisms were probably active. This is important, because in *Pseudomonas* the consumption of organic acids is preferred over the utilization of sugars (59), suggesting that the hierarchy of metabolite preference is different in *C. salexigens*.

Our results show that central metabolism of *C. salexigens* is optimized for high salinity environments, being less efficient at low salt concentrations. Despite this, *C. salexigens* can grow on a wide range of salinities compared with other halophiles, ranging from 0.5 to 3 M NaCl in minimal medium (9). At low salinities, excess glucose cannot be utilized by central metabolism, maybe partly due to some central metabolism enzymes, such as Cs or Gdh, of which the activity levels are lower than the actual glucose consumption fluxes and would act as a bottleneck under these growth conditions. Therefore, the excess glucose is diverted toward overflow metabolites. The high ratio of anaplerotic to catabolic fluxes is a striking fact, especially if we consider that thriving under osmotic stress is usually energetically expensive, especially in microorganisms that use the organic-solutes-in strategy (60, 61).

CONCLUSIONS

This work presents the first experimental description of the metabolism of the highly halotolerant bacterium *C. salexigens*. This microorganism uses the ED pathway for glucose oxidation. Our data show that metabolic efficiency of this bacterium is highly dependent on the salinity of the growth medium. The metabolism of *C. salexigens* is well adapted to support high biosynthetic fluxes toward ectoines. In addition, the existence of multiple routes for the early steps of glucose catabolism might allow it to attain a redox-balanced growth more easily, which is of special relevance when the biosynthetic burden is high. Although these characteristics allow the microorganism to thrive under osmotic stress, at the same time they make it less efficient for growth at low salinity. Overall, this work represents a first insight into the specific metabolic features evolved by halophilic microorganisms to cope with high salinity.

Acknowledgments—We thank Prof. Dan Fraenkel (Harvard Medical School, Boston) for insightful discussions and critical comments on the manuscript. Prof. Helena Santos and Dr. Nuno Borges (Instituto de Tecnología Química e Biológica, Oeiras, Portugal) are gratefully acknowledged for fruitful discussions. Diego Martínez Pérez, M. José Gabaldón, and M. Dolores Pardo from Servicio de Apoyo a la Investigación (Universidad de Murcia) are gratefully acknowledged for their help with NMR and HPLC.

REFERENCES

1. Cayol, J. L., Ducerf, S., Patel, B. K., Garcia, J. L., Thomas, P., and Ollivier, B. (2000) *Thermohalobacter berrensis* gen. nov., sp. nov., a thermophilic, strictly halophilic bacterium from a solar saltern. *Int. J. Syst. Evol. Microbiol.* **50,** 559–564
2. Oren, A., and Mana, L. (2003) Sugar metabolism in the extremely halophilic bacterium *Salinibacter ruber*. *FEMS Microbiol. Lett.* **223,** 83–87
3. Trotsenko, IuA., and Khelenina, V. N. (2002) The biology and osmoadaptation of haloalkaliphilic methanotrophs. *Mikrobiologia* **71,** 149–159
4. Oren, A. (1999) Bioenergetic aspects of halophilism. *Microbiol. Mol. Biol. Rev.* **63,** 334–348
5. Oren, A., Heldal, M., Norland, S., and Galinski, E. A. (2002) Intracellular ion and organic solute concentrations of the extremely halophilic bacterium *Salinibacter ruber*. *Extremophiles* **6,** 491–498
6. Roberts, M. F. (2004) Osmoadaptation and osmoregulation in archaea: update 2004. *Front. Biosci.* **9,** 1999–2019
7. Severin, J., Wohlfarth, A., and Galinslki, E. A. (1992) The predominant role of recently discovered tetrahydropyrimidines for the osmoadaptation of halophilic eubacteria. *J. Gen. Microbiol.* **138,** 1629–1638
8. Pastor, J. M., Salvador, M., Argandoña, M., Bernal, V., Reina-Bueno, M., Csonka, L. N., Iborra, J. L., Vargas, C., Nieto, J. J., and Cánovas, M. (2010) Ectoines in cell stress protection: uses and biotechnological production. *Biotechnol. Adv.* **28,** 782–801
9. Vargas, C., Argandoña, M., Reina-Bueno, M., Rodríguez-Moya, J., Fernández-Aunión, C., and Nieto, J. J. (2008) Unravelling the adaptation responses to osmotic and temperature stress in *Chromohalobacter salexigens*, a bacterium with broad salinity tolerance. *Saline Syst.* **4,** 14
10. Arahal, D. R., García, M. T., Vargas, C., Cánovas, D., Nieto, J. J., and Ventosa, A. (2001) *Chromohalobacter salexigens* sp. nov., a moderately halophilic species that includes *Halomonas elongata* DSM 3043 and ATCC 33174. *Int. J. Syst. Evol. Microbiol.* **51,** 1457–1462
11. Cánovas, D., Vargas, C., Iglesias-Guerra, F., Csonka, L. N., Rhodes, D.,

Ventosa, A., and Nieto, J. J. (1997) Isolation and characterization of salt-sensitive mutants of the moderate halophile halomonas elongata and cloning of the ectoine synthesis genes. *J. Biol. Chem.* **272,** 25794–25801
12. García-Estepa, R., Argandoña, M., Reina-Bueno, M., Capote, N., Iglesias-Guerra, F., Nieto, J. J., and Vargas, C. (2006) The *ectD* gene, which is involved in the synthesis of the compatible solute hydroxyectoine, is essential for thermoprotection of the halophilic bacterium *Chromohalobacter salexigens*. *J. Bacteriol.* **188,** 3774–3784
13. Peters, P. (1990) The biosynthesis of ectoine. *FEMS Microbiol. Lett.* **71,** 157–162
14. Prabhu, J., Schauwecker, F., Grammel, N., Keller, U., and Bernhard, M. (2004) Functional expression of the ectoine hydroxylase gene (*thpD*) from *Streptomyces chrysomallus* in *Halomonas elongata*. *Appl. Environ. Microbiol.* **70,** 3130–3132
15. Cánovas, D., Borges, N., Vargas, C., Ventosa, A., Nieto, J. J., and Santos, H. (1999) Role of N^{γ}-acetyldiaminobutyrate as an enzyme stabilizer and an intermediate in the biosynthesis of hydroxyectoine. *Appl. Environ. Microbiol.* **65,** 3774–3779
16. Copeland, A., O'Connor, K., Lucas, S., Lapidus, A., Berry, K. W., Detter, J. C., Del Rio, T. G., Hammon, N., Dalin, E., Tice, H., Pitluck, S., Bruce, D., Goodwin, L., Han, C., Tapia, R., Saunders, E., Schmutz, J., Brettin, T., Larimer, F., Land, M., Hauser, L., Vargas, C., Nieto, J. J., Kyrpides, N. C., Ivanova, N., Göker, M., Klenk, H.-P., Csonka, L. N., and Woyke, T. (2011) Complete genome sequence of the halophilic and highly halotolerant *Chromohalobacter salexigens* type strain (1H11(T)). *Stand. Genomic Sci.* **5,** 379–388
17. Werner, S., Diekert, G., and Schuster, S. (2010) Revisiting the thermodynamic theory of optimal ATP stoichiometries by analysis of various ATP-producing metabolic pathways. *J. Mol. Evol.* **71,** 346–355
18. Ates, O., Oner, E. T., and Arga, K. Y. (2011) Genome-scale reconstruction of metabolic network for a halophilic extremophile, *Chromohalobacter salexigens* DSM 3043. *BMC Syst. Biol.* **5,** 12
19. Csonka, L. N., O'Connor, K., Larimer, F., Richardson, P., Lapidus, A., Ewing, A., Goodner, B., and Oren, A. (2005) in *Adaptation to Life at High Salt Concentrations in Archaea, Bacteria, and Eukarya* (Gunde-Cimerman, N., Oren, A., and Plemenitas, A., eds) pp. 267–285, Springer, Dordrecht, The Netherlands
20. Vargas, C., Coronado, M. J., Ventosa, A., and Nieto, J. J. (1997) Host range, stability, and compatibility of broad host-range-plasmids and a shuttle vector in moderately halophilic bacteria. Evidence of intrageneric and intergeneric conjugation in moderate halophiles. *Systematic Appl. Microbiol.* **20,** 173–181
21. Peng, L., and Shimizu, K. (2003) Global metabolic regulation analysis for *Escherichia coli* K-12 based on protein expression by two-dimensional electrophoresis and enzyme activity measurement. *Appl. Microbiol. Biotechnol.* **61,** 163–178
22. Aoshima, M., Ishii, M., Yamagishi, A., Oshima, T., and Igarashi, Y. (2003) Metabolic characteristics of an isocitrate dehydrogenase defective derivative of *Escherichia coli* BL21(DE3). *Biotechnol. Bioeng.* **84,** 732–737
23. Buch, A., Archana, G., and Naresh Kumar, G. (2008) Metabolic channeling of glucose toward gluconate in phosphate-solubilizing *Pseudomonas aeruginosa* P4 under phosphorus deficiency. *Res. Microbiol.* **159,** 635–642
24. Van der Werf, M. J., Guettler, M. V., Jain, M. K., and Zeikus, J. G. (1997) Environmental and physiological factors affecting the succinate product ratio during carbohydrate fermentation by *Actinobacillus* sp. 130Z. *Arch. Microbiol.* **167,** 332–342
25. Yagi, T., Toyosato, M., and Soda, K. (1976) Crystalline aspartate aminotransferase from *Pseudomonas striata*. *FEBS Lett.* **61,** 34–37
26. Tesch, M., de Graaf, A. A., and Sahm, H. (1999) *In vivo* fluxes in the ammonium-assimilatory pathways in *Corynebacterium glutamicum* studied by ^{15}N nuclear magnetic resonance. *Appl. Environ. Microbiol.* **65,** 1099–1109
27. Kanehisa, M., and Goto, S. (2000) KEGG: Kyoto encyclopedia of genes and genomes. *Nucleic Acids Res.* **28,** 27–30
28. Caspi, R., Altman, T., Dreher, K., Fulcher, C. A., Subhraveti, P., Keseler, I. M., Kothari, A., Krummenacker, M., Latendresse, M., Mueller, L. A., Ong, Q., Paley, S., Pujar, A., Shearer, A. G., Travers, M., Weerasinghe, D., Zhang, P., and Karp, P. D. (2012) The MetaCyc database of metabolic pathways and enzymes and the BioCyc collection of pathway/genome databases. *Nucleic Acids Res.* **40,** D742–D753
29. Ye, J., McGinnis, S., and Madden, T. L. (2006) BLAST: improvements for better sequence analysis. *Nucleic Acids Res.* **34,** W6–W9
30. Klapa, M. I., Park, S. M., Sinskey, A. J., and Stephanopoulos, G. (1999) Metabolite and isotopomer balancing in the analysis of metabolic cycles: I. Theory. *Biotechnol. Bioeng.* **62,** 375–391
31. Metallo, C. M., Walther, J. L., and Stephanopoulos, G. (2009) Evaluation of ^{13}C isotopic tracers for metabolic flux analysis in mammalian cells. *J. Biotechnol.* **144,** 167–174
32. Cánovas, D., Vargas, C., Csonka, L. N., Ventosa, A., and Nieto, J. J. (1996) Osmoprotectants in *Halomonas elongata*: high affinity betaine transport system and choline-betaine pathway. *J. Bacteriol.* **178,** 7221–7226
33. Entner, N., and Doudoroff, M. (1952) Glucose and gluconic acid oxidation of *Pseudomonas saccharophila*. *J. Biol. Chem.* **196,** 853–862
34. Seo, J.-S., Chong, H., Park, H. S., Yoon, K.-O., Jung, C., Kim, J. J., Hong, J. H., Kim, H., Kim, J.-H., Kil, J.-I., Park, C. J., Oh, H.-M., Lee, J.-S., Jin, S.-J., Um, H.-W., Lee, H.-J., Oh, S.-J., Kim, J. Y., Kang, H. L., Lee, S. Y., Lee, K. J., and Kang, H. S. (2005) The genome sequence of the ethanologenic bacterium *Zymomonas mobilis* ZM4. *Nature Biotechnol.* **23,** 63–68
35. Tang, K.-H., Feng, X., Tang, Y. J., and Blankenship, R. E. (2009) Carbohydrate metabolism and carbon fixation in *Roseobacter denitrificans* OCh114. *PLoS One* **4,** e7233
36. Reshetnikov, A. S., Rozova, O. N., Khmelenina, V. N., Mustakhimov, I. I., Beschastny, A. P., Murrell, J. C., and Trotsenko, Y. A. (2008) Characterization of the pyrophosphate-dependent 6-phosphofructokinase from *Methylococcus capsulatus* Bath. *FEMS Microbiol. Lett.* **288,** 202–210
37. Kemp, R. G., and Tripathi, R. L. (1993) Pyrophosphate-dependent phosphofructo-1-kinase complements fructose 1,6-bisphosphatase but not phosphofructokinase deficiency in *Escherichia coli*. *J. Bacteriol.* **175,** 5723–5724
38. del Castillo, T., Ramos, J. L., Rodríguez-Herva, J. J., Fuhrer, T., Sauer, U., and Duque, E. (2007) Convergent peripheral pathways catalyze initial glucose catabolism in *Pseudomonas putida*: genomic and flux analysis. *J. Bacteriol.* **189,** 5142–5152
39. Castaño-Cerezo, S., Pastor, J. M., Renilla, S., Bernal, V., Iborra, J. L., and Cánovas, M. (2009) An insight into the role of phosphotransacetylase (*pta*) and the acetate/acetyl-CoA node in *Escherichia coli*. *Microb. Cell Fact.* **8,** 54
40. Schwibbert, K., Marin-Sanguino, A., Bagyan, I., Heidrich, G., Lentzen, G., Seitz, H., Rampp, M., Schuster, S. C., Klenk, H.-P., Pfeiffer, F., Oesterhelt, D., and Kunte, H. J. (2011) A blueprint of ectoine metabolism from the genome of the industrial producer *Halomonas elongata* DSM 2581 T. *Environ. Microbiol.* **13,** 1973–1994
41. Goss, T. J., Perez-Matos, A., and Bender, R. A. (2001) Roles of glutamate synthase, *gltBD*, and *gltF* in nitrogen metabolism of *Escherichia coli* and *Klebsiella aerogenes*. *J. Bacterial.* **183,** 6607–6619
42. Sakamoto, N., Kotre, A. M., and Savageau, M. A. (1975) Glutamate dehydrogenase from *Escherichia coli*: purification and properties. *J. Bacteriol.* **124,** 775–783
43. Nicolas, C., Kiefer, P., Letisse, F., Krömer, J., Massou, S., Soucaille, P., Wittmann, C., Lindley, N. D., and Portais, J.-C. (2007) Response of the central metabolism of *Escherichia coli* to modified expression of the gene encoding the glucose-6-phosphate dehydrogenase. *FEBS letters* **581,** 3771–3776
44. Lessie, T. G., and Phibbs, P. V (1984) Alternative pathways of carbohydrate utilization in pseudomonads. *Annu. Rev. Microbiol.* **38,** 359–388
45. Netzer, R., Krause, M., Rittmann, D., Peters-Wendisch, P. G., Eggeling, L., Wendisch, V. F., and Sahm, H. (2004) Roles of pyruvate kinase and malic enzyme in *Corynebacterium glutamicum* for growth on carbon sources requiring gluconeogenesis. *Arch. Microbiol.* **182,** 354–363
46. Kretzschmar, U., Khodaverdi, V., Jeoung, J.-H., and Görisch, H. (2008) Function and transcriptional regulation of the isocitrate lyase in *Pseudomonas aeruginosa*. *Arch. Microbiol.* **190,** 151–158
47. Renilla, S., Bernal, V., Fuhrer, T., Castaño-Cerezo, S., Pastor, J. M., Iborra, J. L., Sauer, U., and Cánovas, M. (2012) Acetate scavenging activity in *Escherichia coli*: interplay of acetyl-CoA synthetase and the PEP-glyoxylate cycle in chemostat cultures. *Appl. Microbiol. Biotechnol.* **95,**

2109–2124
48. Buch, A., Archana, G., and Naresh Kumar, G. (2010) Heterologous expression of phosphoenolpyruvate carboxylase enhances the phosphate solubilizing ability of fluorescent pseudomonads by altering the glucose catabolism to improve biomass yield. *Bioresource Technology* **101,** 679–687
49. Sawyer, M. H., Baumann, P., and Baumann, L. (1977) Pathways of D-fructose and D-glucose catabolism in marine species of *Alcaligenes*, *Pseudomonas marina*, and *Alteromonas communis*. *Arch. Microbiol.* **112,** 169–172
50. Tiwari, N., and Campbell, J. (1969) Enzymatic control of the metabolic activity of *Pseudomonas aeruginosa* grown in glucose or succinate media. *Biochim. Biophys.* **192,** 395–401
51. Hommes, R. W., Postma, P. W., Tempest, D. W., and Neijssel, O. M. (1989) The influence of the culture pH value on the direct glucose oxidative pathway in *Klebsiella pneumoniae* NCTC 418. *Arch. Microbiol.* **151,** 261–267
52. Falb, M., Müller, K., Königsmaier, L., Oberwinkler, T., Horn, P., von Gronau, S., Gonzalez, O., Pfeiffer, F., Bornberg-Bauer, E., and Oesterhelt, D. (2008) Metabolism of halophilic archaea. *Extremophiles* **12,** 177–196
53. Conway, T. (1992) The Entner-Doudoroff pathway: history, physiology, and molecular biology. *FEMS Microbiol. Lett.* **103,** 1–27
54. Ahmed, H., Tjaden, B., Hensel, R., and Siebers, B. (2004) Embden-Meyerhof-Parnas and Entner-Doudoroff pathways in *Thermoproteus tenax*: metabolic parallelism or specific adaptation? *Biochem. Soc. Trans.* **32,** 303–304
55. Dauner, M., Storni, T., and Sauer, U. (2001) *Bacillus subtilis* metabolism and energetics in carbon-limited and excess-carbon chemostat culture. *J. Bacteriol.* **183,** 7308–7317
56. Wendisch, V. F., de Graaf, A. A., Sahm, H., and Eikmanns, B. J. (2000) Quantitative determination of metabolic fluxes during coutilization of two carbon sources: Comparative analyses with *Corynebacterium glutamicum* during growth on acetate and/or glucose. *J. Bacteriol.* **182,** 3088–3096
57. Argandoña, M., Nieto, J. J., Iglesias-Guerra, F., Calderón, M. I., García-Estepa, R., and Vargas, C. (2010) Interplay between iron homeostasis and the osmotic stress response in the halophilic bacterium *Chromohalobacter salexigens*. *Appl. Environ. Microbiol.* **76,** 3575–3589
58. Vemuri, G. N., Altman, E., Sangurdekar, D. P., Khodursky, A. B., and Eiteman, M. A. (2006) Overflow metabolism in *Escherichia coli* during steady-state growth: transcriptional regulation and effect of the redox ratio. *Appl. Environ. Microbiol.* **72,** 3653–3661
59. Rojo, F. (2010) Carbon catabolite repression in *Pseudomonas*: optimizing metabolic versatility and interactions with the environment. *FEMS Microbiol. Rev.* **34,** 658–684
60. Oren, A. (2011) Thermodynamic limits to microbial life at high salt concentrations. *Environ. Microbiol.* **13,** 1908–1923
61. Varela, C. A., Baez, M. E., and Agosin, E. (2004) Osmotic stress response: quantification of cell maintenance and metabolic fluxes in a lysine-overproducing strain of *Corynebacterium glutamicum*. *Appl. Environ. Microbiol.* **70,** 4222–4229